

The New Conformable Methods to Solve Fractional Partial Differential Equations

Halil Hüseyin Avcı¹, Halil Anaç^{*2}

¹Gümüşhane University Graduate Education Institute Department of Mathematical Engineering,
GÜMÜŞHANE

^{*2}Gümüşhane University Torul Vocational School Department of Computer Technologies, GÜMÜŞHANE

(Alınış / Received: 04.07.2023, Kabul / Accepted: 16.08.2023, Online Yayınlanma / Published Online: 31.08.2023)

Keywords

Conformable time-fractional
generalized Burgers
equation,
Conformable Mohand
Adomian decomposition
method,
Conformable Mohand
transform

Abstract: In this article, two novel methods called conformable q-Mohand homotopy analysis transform method (Cq-MHATM) and conformable Mohand Adomian decomposition method (CMADM) are utilized to examine the novel numerical solutions for nonlinear conformable time-fractional generalized Burgers equation with proportional delay. The first of the two new methods suggested, Cq-MHATM, is a hybrid method that combines q-homotopy analysis transform method and Mohand transform in the sense of conformable derivative. The other method, CMADM is also a hybrid method that combines Adomian decomposition method and Mohand transform in the sense of conformable derivative. The computer simulations were worked out to prove that the suggested methods work and are trusted.

Kesirli Mertebeden Kısmi Diferansiyel Denklemlerini Çözmek için Yeni Uyumlu Metotlar

Anahtar Kelimeler

Uyumlu zaman-kesirli
mertebeden genelleştirilmiş
Burgers denklemi,
Uyumlu Mohand Adomian
ayırıştırma metodu,
Uyumlu Mohand dönüşümü

Öz: Bu makalede, uyumlu q-Mohand homotopi analiz dönüşüm yöntemi (Uq-MHADY) ve uyumlu Mohand Adomian ayrıştırma yöntemi (UMAAY) olarak adlandırılan iki yeni yöntem, oransal gecikmeli doğrusal olmayan uyumlu zaman-kesirli mertebeden genelleştirilmiş Burgers denkleminin yeni sayısal çözümlerini incelemek için kullanılmaktadır. Önerilen iki yeni yöntemden ilki olan Uq-MHADY, q-homotopi analiz dönüşüm yöntemi ile uyumlu Mohand dönüşümünün birleşiminden oluşan hibrit bir yöntemdir. Diğer yöntem olan CMADM ise Adomian ayrıştırma yöntemi ile uyumlu Mohand dönüşümünün birleşiminden oluşan hibrit bir yöntemdir. Önerilen yöntemlerin etkin çalıştığını ve güvenilir olduğunu göstermek için bilgisayar simülasyonları yapılmaktadır. Kesin çözümler bulunan çözümlerle karşılaştırıldığında, yeni tekniklerin her ikisinin de basit, güçlü ve oransal gecikmeli doğrusal olmayan uyumlu zaman-kesirli mertebeden kısmi diferansiyel denklemi çözmek için iyi çalıştığını görülmektedir.

*Corresponding Author, email: halilanac0638@gmail.com

1. Introduction

The arbitrary order of fractional calculus (FC) goes beyond the integer order of calculus. It was talked about when the famous scientists Leibniz and L'Hospital first talked to each other around 1695. In recent years, many authors have started to look into fractional calculus because it can be used to give accurate descriptions of many different kinds of nonlinear events. Fractional order differential equations are a type of differential equation that has effects on material properties that are not local and on genetic material. Fractional calculus was studied and described by a number of well-known mathematicians. Their work laid the groundwork for fractional calculus. Now, fractional

partial differential equations are often used to make nonlinear models and study systems that change over time. Fractional-order calculus theory has been linked to many things, such as chaos theory. Fractional differential equations are used to describe the features of natural systems that don't behave in a straight line. We use a number of analytical and numerical methods to solve the time-fractional partial differential equations (TFDEs) that describe nonlinear processes [1-13].

Mohand and Mahgoub [14] created a new integral transform which is called Mohand transform. The mechanics and electrical circuit problems were resolved through the utilization of the Mohand transform. It is provided a method for solving second-order linear Volterra integral equations utilizing the Mohand transform. The utilization of Mohand transform was employed in order to address linear partial integro-differential equations. It is presented the utilization of Mohand transform in the resolution of linear Volterra integro-differential equations. The utilization of Laplace transform for addressing population growth and decay issues is demonstrated [14-19]. The research focuses on the numerical solution of conformable time-fractional partial differential equations with proportional delay defined by

$$\begin{cases} D_t^\alpha w(x, t) = \psi \left(x, w(\rho_0 x, \sigma_0 t), \frac{\partial w(\rho_1 x, \sigma_1 t)}{\partial x}, \dots, \frac{\partial^m w(\rho_m x, \sigma_m t)}{\partial x^m} \right), \\ w^{(k)}(x, 0) = \varphi_k(x), \end{cases} \quad (1)$$

where $\rho_i, \sigma_i \in (0,1)$ for all $i \in N$, φ_k is initial value, ψ differential operator and D_t^α is conformable time-fractional operator.

There aren't many articles in the literature about TFPDEs with proportional delay. These include the Chebyshev pseudospectral method [20], the homotopy analysis method [21], the spectral collocation and waveform relaxation methods [22], and the iterated pseudospectral method [23]. RDTM was used by Abazari and Ganji [24] to find estimated solutions to PDEs. The proportional delay was used in these methods. Abazari and Kilicman [25] used DTM to get analytical solutions to nonlinear integro-differential equations with proportional delay. DTM was used to solve the equations and get these results. Tanthanuch [26] used a method called "group analysis" to solve the "nonhomogeneous inviscid Burgers equation with proportional delay." Sakar et al. [27], Biazar and Ghanbari [28] used the homotopy perturbation method to find analytical solutions to TFPDE with proportional delay. Chen and Wang [29] solved a neutral functional-differential problem with proportional delays using the variational iteration method. Singh and Kumar [30] found an alternative approximation solution to the initial valued autonomous system of TFPDE with proportional delay by using an additional variational iteration method, or AVIM for short. The main goal of this study is to come up with a new method: the conformable q-Mohand homotopy analysis transform method (Cq-MHATM).

Here is a list of the rest of the study: The basic definitions and theorems used are given in the second part. In Section 3, the new conformable fractional numerical methods are presented. In section 4, the application of the suggested methos to the equations is presented. The result is given in section 5.

2. Material and Method

Now let's give the definitions to be used in the study.

Definition 2.1. [31-34] Let a function $f: [0, \infty) \rightarrow \mathbb{R}$. Then, the conformable fractional derivative of f order α is described by

$$T_\alpha(f)(x) = \lim_{\varepsilon \rightarrow 0} \frac{f(x + \varepsilon x^{1-\alpha}) - f(x)}{\varepsilon}, \quad (2)$$

for all $x > 0, \alpha \in (0, 1]$.

Theorem 2.1. [31-32, 34] For $\alpha \in (0, 1], m, n$ be α –differentiable at a point $x > 0$. Then

$$(i) T_\alpha(am + bn) = aT_\alpha(m) + bT_\alpha(n), \text{ for all } a, b \in \mathbb{R}, \quad (3)$$

$$(ii) T_\alpha(x^p) = px^{p-1}, \text{ for all } p \in \mathbb{R}, \quad (4)$$

$$(iii) T_\alpha(\lambda) = 0, \text{ for all constant functions, } m(t) = \lambda, \tag{5}$$

$$(iv) T_\alpha(mn) = mT_\alpha(n) + nT_\alpha(m), \tag{6}$$

$$(v) T_\alpha\left(\frac{m}{n}\right) = \frac{nT_\alpha(m) - mT_\alpha(n)}{n^2}. \tag{7}$$

Definition 2.2. For $0 < \alpha \leq 1$, $f: [0, \infty) \rightarrow \mathbb{R}$ be real valued function. Then, the conformable fractional Mohand transform (CFMT) of order α of f is defined by

$${}_cM_\alpha[f(t)] = R_\alpha(r) = r^2 \int_0^\infty \exp\left(\frac{-rt^\alpha}{\alpha}\right) f(t)t^{\alpha-1} dt. \tag{8}$$

Definition 2.3. For $0 < \alpha \leq 1$, $f: [0, \infty) \rightarrow \mathbb{R}$ be real valued function. The conformable Mohand transform for the conformable fractional-order derivative of the function $f(t)$ is described by

$${}_cM_\alpha[T_\alpha f(t)](v) = rR_\alpha(r) - r^2 f(0). \tag{9}$$

2.1. The New Conformable Fractional Numerical Methods

This section introduces the conformable q-Mohand homotopy analysis transform method and conformable Mohand Adomian decomposition method.

2.1.1. Conformable q-Mohand homotopy analysis transform method

We will introduce a new method. Consider the conformable time-fractional order nonlinear partial differential equation (CTFNPDE) with proportional delay to explain the fundamental idea of Cq-MHATM:

$${}_tT_\alpha w(x, t) + Aw(\rho_i x, \sigma_i t) + Hw(\rho_i x, \sigma_i t) = f(x, t), t > 0, n - 1 < \alpha \leq n, \tag{10}$$

where M is a linear operator, N is a nonlinear operator, $f(x, t)$ is a source term, $\rho_i, \sigma_i \in (0, 1)$ and ${}_tT_\alpha$ is a conformable fractional derivative of order α .

Applying the conformable fractional Mohand transform to Eq. (10) and utilizing the initial condition, then we have

$$rR_\alpha(r) - r^2 w(x, 0) + {}_cM_\alpha[Aw(\rho_i x, \sigma_i t) + Hw(\rho_i x, \sigma_i t)] = {}_cM_\alpha[f(x, t)]. \tag{11}$$

Rearranging the last equation, then we get

$${}_cM_\alpha[w(x, t)] - rw(x, 0) + \frac{1}{r} {}_cM_\alpha[Aw(\rho_i x, \sigma_i t) + Hw(\rho_i x, \sigma_i t)] - \frac{1}{r} {}_cM_\alpha[f(x, t)] = 0. \tag{12}$$

With the help of HAM, we can describe the nonlinear operator for real function $\varphi(x, t; q)$ as follows:

$$\begin{aligned} N[\varphi(x, t; q)] &= {}_cM_\alpha[\varphi(x, t; q)] - r\varphi(x, t; q) (0^+) + \frac{1}{r} ({}_cM_\alpha[A\varphi(\rho_i x, \sigma_i t; q)] \\ &+ {}_cM_\alpha[H\varphi(\rho_i x, \sigma_i t; q)] - \frac{1}{r} {}_cM_\alpha[f(x, t)]), \end{aligned} \tag{13}$$

where $q \in \left[0, \frac{1}{n}\right]$.

We construct a homotopy as follows:

$$(1 - nq) {}_cM_\alpha[\varphi(x, t; q) - w_0(x, t)] = hqH^*(x, t)H[\varphi(\rho_i x, \sigma_i t; q)], \tag{14}$$

where, $h \neq 0$ is an auxiliary parameter and ${}_cM_\alpha$ demonstrates conformable Mohand transform. For $q = 0$ and $q = \frac{1}{n}$, the results of Eq. (14) are as follows:

$$\varphi(x, t; 0) = w_0(x, t), \varphi\left(x, t; \frac{1}{n}\right) = w(x, t). \tag{15}$$

Thus, by amplifying q from 0 to $\frac{1}{n}$, then the solution $\varphi(x, t; q)$ converges from $w_0(x, t)$ to the solution $w(x, t)$. Using the Taylor theorem around q and then expanding $\varphi(x, t; q)$, we get

$$\varphi(x, t; q) = w_0(x, t) + \sum_{i=1}^{\infty} w_m(x, t)q^m, \tag{16}$$

where

$$w_m(x, t) = \frac{1}{m!} \frac{\partial^m \varphi(x, t; q)}{\partial q^m} \Big|_{q=0}. \tag{17}$$

Eq. (16) converges at $q = \frac{1}{n}$ for the appropriate $w_0(x, t)$, n and h . Then, we have

$$w(x, t) = w_0(x, t) + \sum_{m=1}^{\infty} w_m(x, t) \left(\frac{1}{n}\right)^m. \tag{18}$$

If we differentiate the zeroth order deformation Eq. (14) m -times with respect to q and we divide by $m!$, respectively, then for $q = 0$, we acquire

$${}_cM_\alpha[w_m(x, t) - k_m w_{m-1}(x, t)] = hH^*(x, t)\mathcal{R}_m(\vec{w}_{m-1}), \tag{19}$$

where the vectors are described by

$$\vec{w}_m = \{w_0(x, t), w_1(x, t), \dots, w_m(x, t)\}. \tag{20}$$

Applying the inverse conformable fractional Mohand transform to Eq. (20), we get

$$w_m(x, t) = k_m w_{m-1}(x, t) + h({}_cM_\alpha)^{-1}[H^*(x, t)\mathcal{R}_m(\vec{w}_{m-1})], \tag{21}$$

where

$$\begin{aligned} \mathcal{R}_m(\vec{w}_{m-1}) = & {}_cM_\alpha[w_{m-1}(x, t)] - \left(1 - \frac{k_m}{n}\right)rw_0(x, t) + \frac{1}{r}{}_cM_\alpha[Aw_{m-1}(\rho_i x, \sigma_i t) \\ & + H_{m-1}(x, t) - f(x, t)], \end{aligned} \tag{22}$$

and

$$k_m = \begin{cases} 0, & m \leq 1, \\ n, & m > 1. \end{cases} \tag{23}$$

Here, H_m^* is homotopy polynomial and presented by

$$H_m^* = \frac{1}{m!} \frac{\partial^m \varphi(x, t; q)}{\partial q^m} \Big|_{q=0} \text{ and } \varphi(x, t; q) = \varphi_0 + q\varphi_1 + q^2\varphi_2 + \dots. \tag{24}$$

Using Eqs. (21) - (22), we get

$$w_m(x, t) = (k_m + h)w_{m-1}(x, t) - \left(1 - \frac{k_m}{n}\right)rw_0(x, t) + h({}_cM_\alpha)^{-1} \left[\left(\frac{1}{r}{}_cM_\alpha[Aw_{m-1}(\rho_i x, \sigma_i t) \right. \right.$$

$$+H_{m-1}(x, t) - f(x, t)]. \tag{25}$$

When Cq-MHATM is used, the series solution is given by

$$w(x, t) = \sum_{m=0}^{\infty} w_m(x, t) \left(\frac{1}{n}\right)^m. \tag{26}$$

2.1.2. Conformable Mohand Adomian decomposition method

We analyze the CTFNPDE with proportional delay in Eq. (10):

Applying the conformable fractional Mohand transform to Eq. (10) and using the initial condition, then we have

$$rR_{\alpha}(r) - r^2w(x, 0) + {}_cM_{\alpha}[Aw(\rho_i x, \sigma_i t) + Hw(\rho_i x, \sigma_i t)] = {}_cM_{\alpha}[f(x, t)]. \tag{27}$$

When Eq. (27) is rearranged, it is obtained as

$$r {}_cM_{\alpha}[w(x, t)] - rw(x, 0) + \frac{1}{r} {}_cM_{\alpha}[Aw(\rho_i x, \sigma_i t) + Hw(\rho_i x, \sigma_i t)] - \frac{1}{r} {}_cM_{\alpha}[f(x, t)] = 0. \tag{28}$$

When the inverse conformable fractional Mohand transform is implemented to both sides of Eq. (28), we have

$$w(x, t) = A(x, t) - ({}_cM_{\alpha})^{-1} \left\{ \frac{1}{r} {}_cM_{\alpha}[Aw(\rho_i x, \sigma_i t) + Hw(\rho_i x, \sigma_i t)] \right\}. \tag{29}$$

where the term $A(x, t)$ emerges from the in-homogeneous term and initial conditions. Now, assume that the infinite series solution is of the form:

$$w(x, t) = \sum_{n=0}^{\infty} w_n(x, t). \tag{30}$$

Now, by using Eqs. (29)-(30), we get

$$\sum_{n=0}^{\infty} w_n(x, t) = A(x, t) - ({}_cM_{\alpha})^{-1} \left\{ \frac{1}{r} {}_cM_{\alpha} \left[A \sum_{n=0}^{\infty} w_n(\rho_i x, \sigma_i t) + \sum_{n=0}^{\infty} B_n(w_n(\rho_i x, \sigma_i t)) \right] \right\}, \tag{31}$$

where $B_n(w_n)$ is Adomian polynomial and that denotes the nonlinear term $Hw(\rho_i x, \sigma_i t)$. By comparing both of sides of Eq. (31), we have

$$w_0(x, t) = A(x, t), \tag{32}$$

$$w_1(x, t) = -({}_cM_{\alpha})^{-1} \left\{ \frac{1}{r} {}_cM_{\alpha}[w_0(\rho_i x, \sigma_i t) + B_0] \right\}, \tag{33}$$

$$w_2(x, t) = -({}_cM_{\alpha})^{-1} \left\{ \frac{1}{r} {}_cM_{\alpha}[w_1(\rho_i x, \sigma_i t) + B_1] \right\}, \tag{34}$$

⋮

Similarly, we obtain the general recursive relation by

$$w_{n+1}(x, t) = -({}_cM_{\alpha})^{-1} \left\{ \frac{1}{r} {}_cM_{\alpha}[w_n(\rho_i x, \sigma_i t) + B_n] \right\}, m \geq 1. \tag{35}$$

Finally, the approximate solution $w(x, t)$ is given by

$$w(x, t) = \sum_{n=0}^{\infty} w_n(x, t). \tag{36}$$

3. Results

This section will provide illustrations of the conformable time-fractional generalized Burgers equation with proportional delay.

Example 3.1. [27, 30] Consider the conformable time-fractional generalized Burgers equation with proportional delay

$$\frac{\partial^\alpha w(x, t)}{\partial t^\alpha} = \frac{\partial^2 w(x, t)}{\partial x^2} + w\left(\frac{x}{2}, \frac{t}{2}\right) \frac{\partial w\left(x, \frac{t}{2}\right)}{\partial x} + \frac{1}{2} w(x, t), \tag{37}$$

where $x, t \in [0,1], 0 < \alpha \leq 1$, subject to initial condition

$$w(x, 0) = x. \tag{38}$$

Case (i) Cq-MHATM solution

Implementing the conformable fractional Mohand transform to Eq. (37) and using Eq. (38), then we get

$${}_cM_\alpha[w(x, t)] = r w(x, 0) + \frac{1}{r} {}_cM_\alpha \left[\frac{\partial^2 w(x, t)}{\partial x^2} + w\left(\frac{x}{2}, \frac{t}{2}\right) \frac{\partial w\left(x, \frac{t}{2}\right)}{\partial x} + \frac{1}{2} w(x, t) \right]. \tag{39}$$

We define the nonlinear operators by using Eq. (39), as

$$N[\varphi(x, t; q)] = {}_cM_\alpha[\varphi(x, t; q)] - r x - \frac{1}{r} {}_cM_\alpha \left[\frac{\partial^2 \varphi(x, t; q)}{\partial x^2} + \varphi\left(\frac{x}{2}, \frac{t}{2}; q\right) \frac{\partial \varphi\left(x, \frac{t}{2}; q\right)}{\partial x} + \frac{1}{2} \varphi\left(\frac{x}{2}, \frac{t}{2}; q\right) \right]. \tag{40}$$

When the suggested algorithm is applied, the $m - th$ order deformation equations are described by

$${}_cM_\alpha[w_m(x, t) - k_m w_{m-1}(x, t)] = h \mathcal{R}_m[\vec{w}_{m-1}], \tag{41}$$

where

$$\begin{aligned} \mathcal{R}_m[\vec{w}_{m-1}] = & {}_cM_\alpha[\vec{w}_{m-1}(x, t)] - \left(1 - \frac{k_m}{n}\right) r x - \frac{1}{r} {}_cM_\alpha \left[\frac{\partial^2 w_{m-1}(x, t; q)}{\partial x^2} + \sum_{r=0}^{m-1} w_r\left(\frac{x}{2}, \frac{t}{2}\right) \right. \\ & \left. \times \frac{\partial w_{1-r}\left(x, \frac{t}{2}\right)}{\partial x} + \frac{1}{2} w_{m-1}\left(\frac{x}{2}, \frac{t}{2}\right) \right]. \end{aligned} \tag{42}$$

On applying inverse conformable Mohand transform to Eq. (41), then we have

$$w_m(x, t) = k_m w_{m-1}(x, t) + h ({}_cM_\alpha)^{-1} \{ \mathcal{R}_m[\vec{w}_{m-1}] \}. \tag{43}$$

By the use of initial condition, then we get

$$w_0(x, t) = x. \tag{44}$$

To find the value of $w_1(x, t)$, putting $m = 1$ in Eq. (43), then we obtain

$$w_1(x, t) = -xh \frac{t^\alpha}{\alpha}. \tag{45}$$

In the same way, if we put $m = 2$ in Eq. (43), we can obtain the value of $w_2(x, t)$

$$w_2(x, t) = -(n + h) \left(hx \frac{t^\alpha}{\alpha} \right) + \left(\frac{5xh^2t^{2\alpha}}{82^\alpha\alpha^2} \right). \tag{46}$$

In this way, the other terms can be found. So, the Cq-MHATM solution of the equation is given by

$$w(x, t) = w_0(x, t) + \sum_{m=1}^{\infty} w_m(x, t) \left(\frac{1}{n} \right)^m. \tag{47}$$

If we put $\alpha = 1, n = 1, h = -1$ in Eq. (46), then the obtained results $\sum_{m=1}^M w_m(x, t) \left(\frac{1}{n} \right)^m$ converges to the exact solution $w(x, t) = xe^t$ of the equation when $M \rightarrow \infty$.

Case (ii) CMADM solution

Applying the conformable fractional Mohand transform to Eq. (37) and using Eq. (38), then we get

$${}_cM_\alpha[w(x, t)] = rw(x, 0) + \frac{1}{r} {}_cM_\alpha \left[\frac{\partial^2 w(x, t)}{\partial x^2} + w \left(\frac{x}{2}, \frac{t}{2} \right) \frac{\partial w \left(x, \frac{t}{2} \right)}{\partial x} + \frac{1}{2} w(x, t) \right]. \tag{48}$$

Applying the inverse fractional Mohand transform to Eq (48), then we obtain

$$w(x, t) = x + ({}_cM_\alpha)^{-1} \left\{ \frac{1}{r} {}_cM_\alpha \left[\frac{\partial^2 w(x, t)}{\partial x^2} + w \left(\frac{x}{2}, \frac{t}{2} \right) \frac{\partial w \left(x, \frac{t}{2} \right)}{\partial x} + \frac{1}{2} w(x, t) \right] \right\}. \tag{49}$$

Now, assume that the infinite series solution is of the form:

$$w(x, t) = \sum_{n=0}^{\infty} w_n(x, t). \tag{50}$$

Using the ADM procedure, then we obtain

$$w_0(x, t) = x, \tag{51}$$

$$w_{s+1}(x, t) = ({}_cM_\alpha)^{-1} \left[\frac{1}{r} {}_cM_\alpha \left[\frac{\partial^2 w_s(x, t)}{\partial x^2} + w_s \left(\frac{x}{2}, \frac{t}{2} \right) \frac{\partial w_s \left(x, \frac{t}{2} \right)}{\partial x} + \frac{1}{2} w_s(x, t) \right], s = 0, 1, 2, \dots \right] \tag{52}$$

For $s = 0$ in Eq. (52), we obtain

$$w_1(x, t) = ({}_cM_\alpha)^{-1} \left[\frac{1}{r} {}_cM_\alpha \left[\frac{\partial^2 w_0(x, t)}{\partial x^2} + w_0 \left(\frac{x}{2}, \frac{t}{2} \right) \frac{\partial w_0 \left(x, \frac{t}{2} \right)}{\partial x} + \frac{1}{2} w_0(x, t) \right] \right] \\ = x \frac{t^\alpha}{\alpha}, \tag{53}$$

For $s = 1$ in Eq. (52), we obtain

$$w_2(x, t) = -({}_cM_\alpha)^{-1} \left[\frac{1}{r} {}_cM_\alpha \left[\frac{\partial^2 w_1(x, t)}{\partial x^2} + w_0\left(\frac{x}{2}, \frac{t}{2}\right) \frac{\partial w_1\left(x, \frac{t}{2}\right)}{\partial x} + w_1\left(\frac{x}{2}, \frac{t}{2}\right) \frac{\partial w_0\left(x, \frac{t}{2}\right)}{\partial x} + \frac{1}{2} w_1(x, t) \right] \right] = \frac{5xh^2t^{2\alpha}}{82^\alpha \alpha^2}. \tag{54}$$

As a result, we obtain

$$w(x, t) = \sum_{n=0}^{\infty} w_n(x, t) = w_0(x, t) + w_1(x, t) + w_2(x, t) + \dots = x + x \frac{t^\alpha}{\alpha} + \frac{5xh^2t^{2\alpha}}{82^\alpha \alpha^2} + \dots \tag{55}$$

Substituting $\alpha = 1$ in Eq. (55), then CMADM solution is reduced as

$$w(x, t) = x \left[1 + t + \frac{5t^2}{8.2!} + \dots \right]. \tag{57}$$

This result converges to the exact solution in a closed form:

$$w(x, t) = xe^t. \tag{58}$$

Figure 1 shows the graphs of Cq-MHATM, exact solution and absolute error.

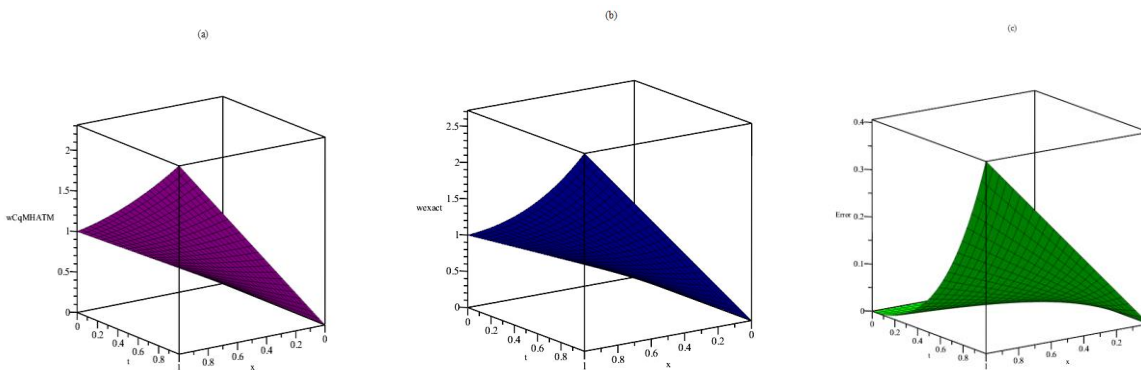


Figure 1. (a) Nature of Cq-MHATM solution **(b)** Nature of exact solution **(c)** Nature of absolute error= $|w_{exact} - w_{Cq-MHATM}|$ at $h = -1, n = 1, \alpha = 1$.

The 3D graphs of CMADM, exact solution, and absolute error are depicted in Figure 2.

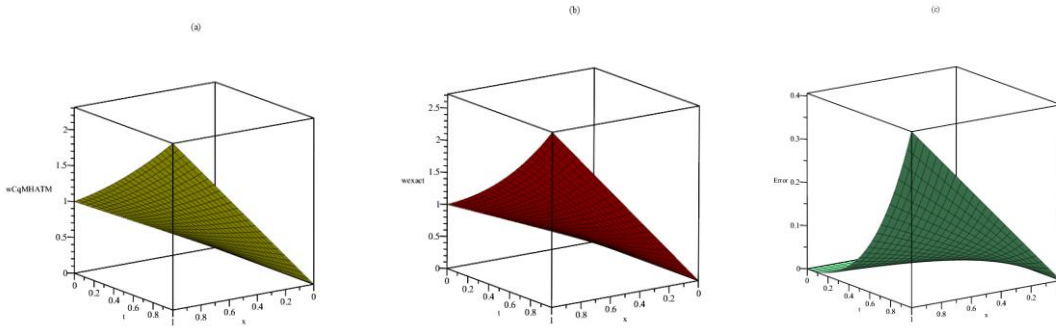


Figure 2. (a) Nature of CqMADM solution (b) Nature of exact solution (c) Nature of absolute error= $|w_{exact} - w_{CMADM}|$ at $\alpha = 1$.

Figure 3 depicts comparison plots of Cq-MHATM, CMADM, and exact solutions for distinct α values.

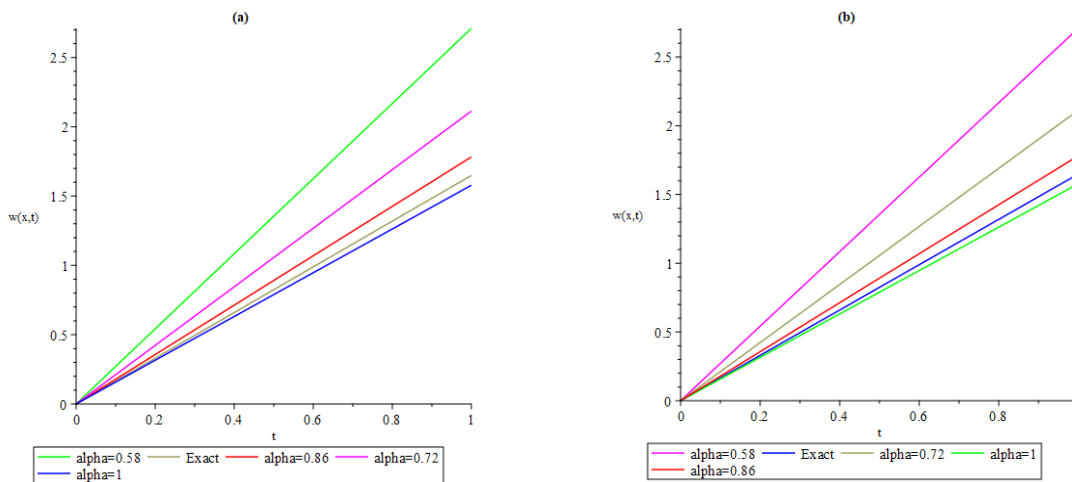


Figure 3. The comparison of the Cq-MHATM solutions and exact solution (b) The comparison of the CMADM solutions and exact solution at $h = -1, n = 1, t = 0.5$ with different α .

A comparison of the absolute error between Cq-MHATM, CMADM and HPM [27] for Eq. (37) with $\alpha = 1$ is presented in Table 1.

Table 1. Comparison of absolute error between Cq-MHATM, CMADM, and HPM [27] for Eq. (37) with $\alpha = 1$.

| x | | t | | | |
|-----------------|-------------|----------------------|----------------------|----------------------|----------------------|
| | | 0.025 | 0.050 | 0.075 | 0.1 |
| Cq-MHATM | 0.25 | 1.0×10^{-9} | 1.6×10^{-8} | 8.1×10^{-8} | 2.5×10^{-7} |
| CMADM | | 1.0×10^{-9} | 1.6×10^{-8} | 8.1×10^{-8} | 2.5×10^{-7} |
| HPM | | 1.0×10^{-9} | 1.6×10^{-8} | 8.1×10^{-8} | 2.5×10^{-7} |
| Cq-MHATM | 0.50 | 4.0×10^{-9} | 6.4×10^{-6} | 3.2×10^{-7} | 1.0×10^{-6} |
| CMADM | | 4.0×10^{-9} | 6.4×10^{-6} | 3.2×10^{-7} | 1.0×10^{-6} |
| HPM | | 4.0×10^{-9} | 6.4×10^{-6} | 3.2×10^{-7} | 1.0×10^{-6} |
| Cq-MHATM | 0.75 | 9.1×10^{-9} | 1.4×10^{-7} | 7.3×10^{-7} | 2.2×10^{-6} |
| CMADM | | 9.1×10^{-9} | 1.4×10^{-7} | 7.3×10^{-7} | 2.2×10^{-6} |
| HPM | | 9.1×10^{-9} | 1.4×10^{-7} | 7.3×10^{-7} | 2.2×10^{-6} |

Example 3.2. [27, 30] Consider the conformable time-fractional generalized Burgers equation with proportional delay

$$\frac{\partial^\alpha w(x, t)}{\partial t^\alpha} = \frac{\partial^2 w\left(\frac{x}{2}, \frac{t}{2}\right)}{\partial x^2} \frac{\partial w\left(\frac{x}{2}, \frac{t}{2}\right)}{\partial x} - \frac{1}{8} \frac{\partial w(x, t)}{\partial x} - w(x, t), \tag{59}$$

where $x, t \in [0,1], 0 < \alpha \leq 1$, subject to initial condition

$$w(x, 0) = x^2. \tag{60}$$

Case (i) Cq-MHATM solution

Implementing the conformable fractional Mohand transform to Eq. (59) and using Eq. (60), then we get

$${}_cM_\alpha[w(x, t)] = r w(x, 0) - \frac{1}{r} {}_cM_\alpha \left[\frac{\partial^2 w \left(\frac{x}{2}, \frac{t}{2} \right)}{\partial x^2} \frac{\partial w \left(\frac{x}{2}, \frac{t}{2} \right)}{\partial x} - \frac{1}{8} \frac{\partial w(x, t)}{\partial x} - w(x, t) \right]. \tag{61}$$

We define the nonlinear operators by using Eq. (61), as

$$N[\varphi(x, t; q)] = {}_cM_\alpha[\varphi(x, t; q)] - r x^2 - \frac{1}{r} {}_cM_\alpha \left[\frac{\partial^2 w \left(\frac{x}{2}, \frac{t}{2} \right)}{\partial x^2} \frac{\partial w \left(\frac{x}{2}, \frac{t}{2} \right)}{\partial x} - \frac{1}{8} \frac{\partial w(x, t)}{\partial x} - w(x, t) \right]. \tag{62}$$

By applying the suggested algorithm, the $m - th$ order deformation equations are described by

$${}_cM_\alpha[w_m(x, t) - k_m w_{m-1}(x, t)] = h \mathcal{R}_m[\bar{w}_{m-1}], \tag{63}$$

where

$$\mathcal{R}_m[\bar{w}_{m-1}] = {}_cM_\alpha[\bar{w}_{m-1}(x, t)] - \left(1 - \frac{k_m}{n} \right) r x^2 - \frac{1}{r} {}_cM_\alpha \left[\sum_{r=0}^{m-1} \frac{\partial^2 w_r \left(\frac{x}{2}, \frac{t}{2} \right)}{\partial x^2} \frac{\partial w_{1-r} \left(\frac{x}{2}, \frac{t}{2} \right)}{\partial x} - \frac{1}{8} \frac{\partial w_{m-1}(x, t)}{\partial x} - w_{m-1}(x, t) \right]. \tag{64}$$

On applying inverse conformable fractional Mohand transform to Eq. (63), then we have

$$w_m(x, t) = k_m w_{m-1}(x, t) + h ({}_cM_\alpha)^{-1} \{ \mathcal{R}_m[\bar{w}_{m-1}] \}. \tag{65}$$

By the use of initial condition, then we get

$$w_0(x, t) = x^2. \tag{66}$$

To find the value of $w_1(x, t)$, putting $m = 1$ in Eq. (65), then we obtain

$$w_1(x, t) = h x^2 \frac{t^\alpha}{\alpha}. \tag{67}$$

In the same way, if we put $m = 2$ in Eq. (65), we can obtain the value of $w_2(x, t)$

$$w_2(x, t) = (n + h) \left(h x^2 \frac{t^\alpha}{\alpha} \right) - h^2 \left(\frac{x}{2^{\alpha+1}} - \frac{x}{4} - x^2 \right) \frac{t^{2\alpha}}{2\alpha^2}. \tag{68}$$

In this way, the other terms can be found. So, the Cq-MHATM solution of the equation is given by

$$w(x, t) = w_0(x, t) + \sum_{m=1}^{\infty} w_m(x, t) \left(\frac{1}{n} \right)^m. \tag{69}$$

If we put $\alpha = 1, n = 1, h = -1$ in Eq. (68), then the obtained results $\sum_{m=1}^M w_m(x, t) \left(\frac{1}{n} \right)^m$ converges to the exact solution $w(x, t) = x^2 e^{-t}$ of the equation when $M \rightarrow \infty$.

Case (ii) CMADM solution

Applying the conformable fractional Mohand transform to Eq. (59) and using Eq. (60), then we get

$${}_cM_\alpha[w(x, t)] = rw(x, 0) - \frac{1}{r} {}_cM_\alpha \left[\frac{\partial^2 w \left(\frac{x}{2}, \frac{t}{2} \right)}{\partial x^2} \frac{\partial w \left(\frac{x}{2}, \frac{t}{2} \right)}{\partial x} - \frac{1}{8} \frac{\partial w(x, t)}{\partial x} - w(x, t) \right]. \tag{70}$$

Applying the inverse fractional Mohand transform to Eq (70), then we obtain

$$w(x, t) = x^2 - ({}_cM_\alpha)^{-1} \left\{ \frac{1}{r} {}_cM_\alpha \left[\frac{\partial^2 w \left(\frac{x}{2}, \frac{t}{2} \right)}{\partial x^2} \frac{\partial w \left(\frac{x}{2}, \frac{t}{2} \right)}{\partial x} - \frac{1}{8} \frac{\partial w(x, t)}{\partial x} - w(x, t) \right] \right\}. \tag{71}$$

Now, assume that the infinite series solution is of the form:

$$w(x, t) = \sum_{n=0}^{\infty} w_n(x, t). \tag{72}$$

Using the ADM procedure, then we obtain

$$w_0(x, t) = x^2, \tag{73}$$

$$w_{s+1}(x, t) = -({}_cM_\alpha)^{-1} \left[\frac{1}{r} {}_cM_\alpha \left[\frac{\partial^2 w_s \left(\frac{x}{2}, \frac{t}{2} \right)}{\partial x^2} \frac{\partial w_s \left(\frac{x}{2}, \frac{t}{2} \right)}{\partial x} - \frac{1}{8} \frac{\partial w_s(x, t)}{\partial x} - w_s(x, t) \right] \right], s = 0, 1, 2, \dots \tag{74}$$

For $s = 0$ in Eq. (74), we obtain

$$\begin{aligned} w_1(x, t) &= -({}_cM_\alpha)^{-1} \left[\frac{1}{r} {}_cM_\alpha \left[\frac{\partial^2 w_0 \left(\frac{x}{2}, \frac{t}{2} \right)}{\partial x^2} \frac{\partial w_0 \left(\frac{x}{2}, \frac{t}{2} \right)}{\partial x} - \frac{1}{8} \frac{\partial w_0(x, t)}{\partial x} - w_0(x, t) \right] \right] \\ &= -x^2 \frac{t^\alpha}{\alpha}. \end{aligned} \tag{75}$$

For $s = 1$ in Eq. (74), we obtain

$$\begin{aligned} w_2(x, t) &= -({}_cM_\alpha)^{-1} \left[\frac{1}{r} {}_cM_\alpha \left[\frac{\partial^2 w_1 \left(\frac{x}{2}, \frac{t}{2} \right)}{\partial x^2} \frac{\partial w_1 \left(\frac{x}{2}, \frac{t}{2} \right)}{\partial x} - \frac{1}{8} \frac{\partial w_1(x, t)}{\partial x} - w_1(x, t) \right] \right] \\ &= -\left(\frac{x}{2^{\alpha+1}} - \frac{x}{4} - x^2 \right) \frac{t^{2\alpha}}{2\alpha^2}. \end{aligned} \tag{76}$$

As a result, we obtain

$$\begin{aligned} w(x, t) &= \sum_{n=0}^{\infty} w_n(x, t) = w_0(x, t) + w_1(x, t) + w_2(x, t) + \dots \\ &= x^2 - x^2 \frac{t^\alpha}{\alpha} - \left(\frac{x}{2.2^\alpha} - \frac{x}{4} - x^2 \right) \frac{t^{2\alpha}}{2\alpha^2} + \dots \end{aligned} \tag{77}$$

Substituting $\alpha = 1$ in Eq. (78), then CMADM solution is reduced as

$$w(x, t) = x^2 \left[1 - t + \frac{t^2}{2!} - \dots \right]. \tag{78}$$

This result converges to the exact solution in a closed form:

$$w(x, t) = x^2 e^{-t}. \tag{79}$$

Figure 4 shows the graphs of Cq-MHATM, exact solution and absolute error.

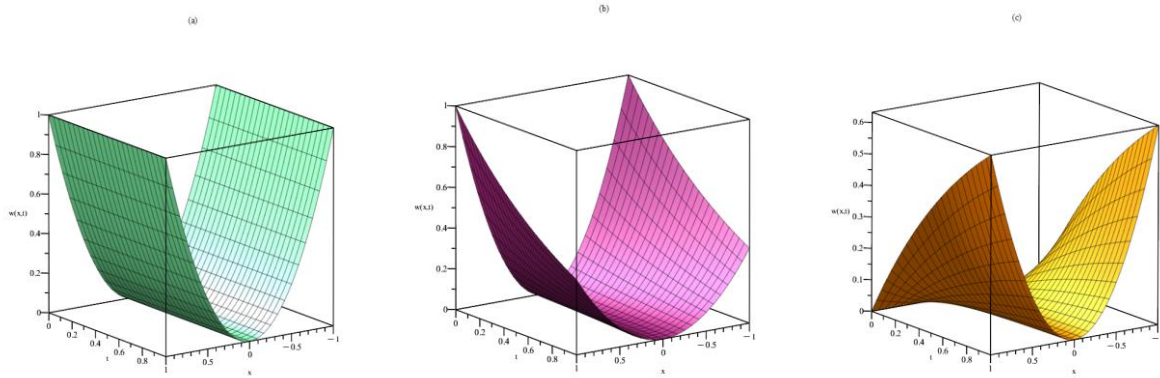


Figure 4. (a) Nature of Cq-MHATM solution (b) Nature of exact solution (c) Nature of absolute error= $|w_{exact} - w_{Cq-MHATM}|$ at $h = -1, n = 1, \alpha = 1$.

The graphs of CMADM, exact solution, and absolute error are depicted in Figure 5.

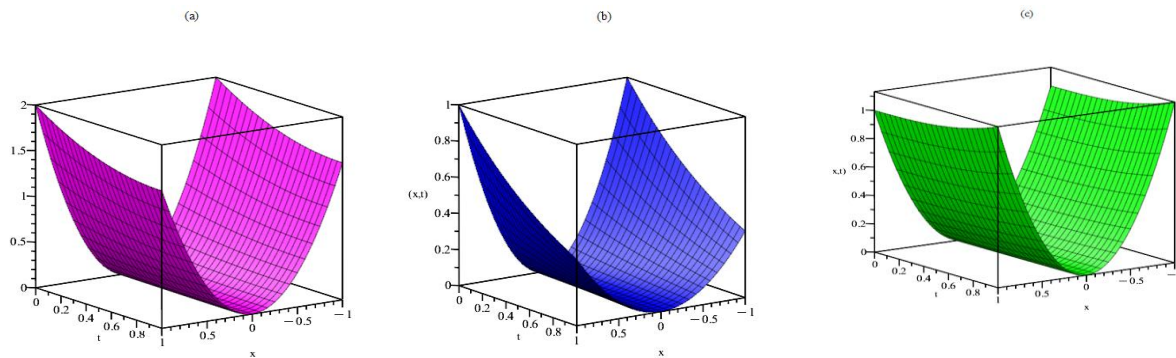


Figure 5. (a) Nature of CMADM solution (b) Nature of exact solution (c) Nature of absolute error= $|w_{exact} - w_{CMADM}|$ at $\alpha = 1$.

Figure 6 depicts comparison plots of Cq-MHATM, CMADM, and exact solutions for distinct α values.

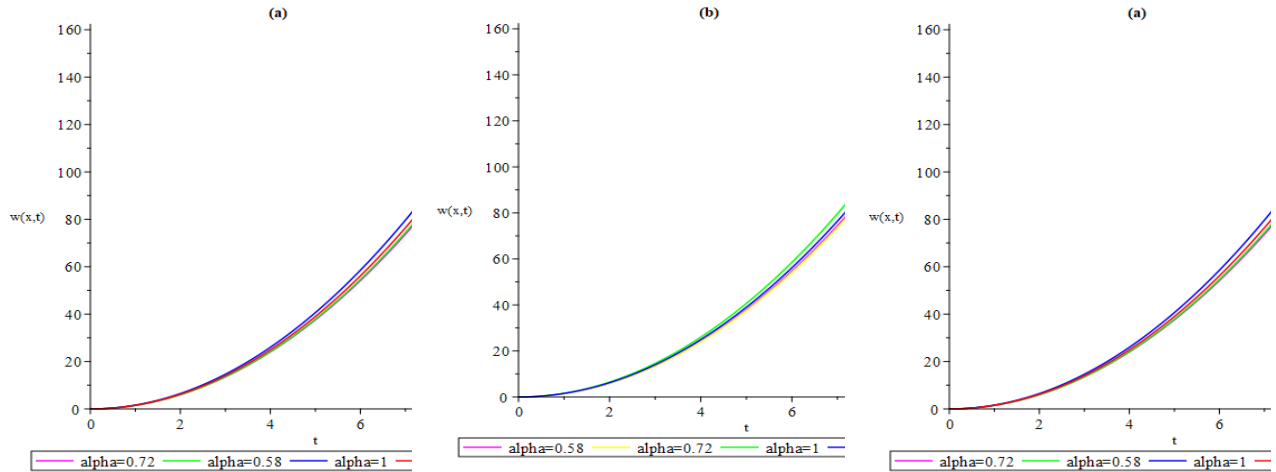


Figure 6. The comparison of the Cq-MHATM solutions and exact solution **(b)** The comparison of the CMADM solutions and exact solution at $h = -1, n = 1, t = 0.5$ with different α .

Table 2 presents a comparison of the absolute error for Eq. (59) with $\alpha = 1$ between Cq-MHATM, CMADM, and HPM [27].

Table 2. Comparison of absolute error between Cq-MHATM, CMADM, and HPM [27] for Eq. (59) with $\alpha = 1$.

| x | | t | | | |
|-----------------|-------------|----------------------|----------------------|----------------------|----------------------|
| | | 0.025 | 0.050 | 0.075 | 0.1 |
| Cq-MHATM | 0.25 | 1.6×10^{-7} | 1.2×10^{-6} | 4.3×10^{-6} | 1.0×10^{-5} |
| | | 1.6×10^{-7} | 1.2×10^{-6} | 4.3×10^{-6} | 1.0×10^{-5} |
| | | 1.6×10^{-7} | 1.2×10^{-6} | 4.3×10^{-6} | 1.0×10^{-5} |
| Cq-MHATM | 0.50 | 6.4×10^{-7} | 5.1×10^{-6} | 1.7×10^{-5} | 4.0×10^{-5} |
| | | 6.4×10^{-7} | 5.1×10^{-6} | 1.7×10^{-5} | 4.0×10^{-5} |
| | | 6.4×10^{-7} | 5.1×10^{-6} | 1.7×10^{-5} | 4.0×10^{-5} |
| Cq-MHATM | 0.75 | 1.4×10^{-6} | 1.1×10^{-5} | 3.8×10^{-5} | 9.1×10^{-5} |
| | | 1.4×10^{-6} | 1.1×10^{-5} | 3.8×10^{-5} | 9.1×10^{-5} |
| | | 1.4×10^{-6} | 1.1×10^{-5} | 3.8×10^{-5} | 9.1×10^{-5} |

4. Discussion and Conclusion

Table 1 evaluates the absolute error comparison between Cq-HATM, CSHPM, and HPM for Eq. (37) with $\alpha = 1$ for the nonlinear conformable time-fractional generalized Burgers equation (CTFGBE) with proportional delay. The 3D graphs of Cq-MHATM, exact solution, and absolute error are depicted in Figure 1. Figure 2 depicts 3D graphs of CMADM, exact solution, and absolute error. Figure 3 depicts a comparison of Cq-MHATM, CMADM, and exact solutions in 2D plots for various α values. Table 2 presents an assessment of the absolute error comparison among Cq-HATM, CSHPM, and HPM methods for Eq. (59) with $\alpha = 1$, applied to the nonlinear conformable time-fractional generalized Burgers equation (CTFGBE) with proportional delay. Figure 4 illustrates the three-dimensional plots of Cq-MHATM, the exact solution, and the absolute error. The graphical representation in Figure 5 illustrates three-dimensional graphs of the CMADM, the exact solution, and the absolute error. The 2D plots in Figure 6 present a comparison of the solutions for Cq-MHATM, CMADM, and exact solution with respect to various α values. The study found that the techniques presented in Tables 1-2 produced equivalent results to those obtained through the use of HPM. The results indicate that the techniques presented in Table 6 produced equivalent results to those obtained through the use of HPM.

This study investigates the behavior of CTFGBE with proportional delay using Cq-MHATM and CMADM. Furthermore, the MAPLE software has been utilized to produce 2D and 3D graphs that depict the solutions to Eqs. (37)-(59) for diverse values of α . Variations in the construction of the surface graphs for Eqs. (37)-(59) have been observed. Variations in the construction of the surface for Eqs. (37)-(59) have been noted. The research revealed that the methodologies illustrated in Tables 1-2 yielded outcomes that were comparable to those achieved by employing HPM, with t as the independent variable and x held constant.

The efficacy and benefits of the newly developed approach for addressing nonlinear conformable TFPDEs with proportional delay have been noted.

References

- [1] Miller, K. S., Ross, B. 1993. An introduction to the fractional calculus and fractional differential equations, Wiley, New York, 376 p.
- [2] Podlubny, I. 1999. Fractional differential equations, mathematics in science and engineering, Academic Press, New York, 365 p.
- [3] Baleanu, D., Diethelm, K., Scalas, E., Trujillo, J. J. 2012. *Fractional calculus: models and numerical methods*, World Scientific, London, 476 p.
- [4] Povstenko, Y. 2015. Linear fractional diffusion-wave equation for scientists and engineers. Birkhäuser, Switzerland, 460 p.
- [5] Ala, V. 2022. New exact solutions of space-time fractional Schrödinger-Hirota equation. Bulletin of the Karaganda university Mathematics series, 107(3), 17-24.
- [6] Ala, V. 2023. Exact Solutions of Nonlinear Time Fractional Schrödinger Equation with Beta- Derivative. Fundamentals of Contemporary Mathematical Sciences, 4(1), 1-8.
- [7] Baleanu, D., Wu, G. C., Zeng, S. D. 2017. Chaos analysis and asymptotic stability of generalized Caputo fractional differential equations. Chaos, Solitons & Fractals, 102, 99-105.
- [8] Sweilam, N. H., Abou Hasan, M. M., Baleanu, D. 2017. New studies for general fractional financial models of awareness and trial advertising decisions. Chaos, Solitons & Fractals, 104, 772-784.
- [9] Liu, D. Y., Gibaru, O., Perruquetti, W., Laleg-Kirati, T. M. 2015. Fractional order differentiation by integration and error analysis in noisy environment. *IEEE Transactions on Automatic Control*, 60(11), 2945-2960.
- [10] Esen, A., Sulaiman, T. A., Bulut, H., Baskonus, H. M. 2018. Optical solitons to the space-time fractional (1+1)-dimensional coupled nonlinear Schrödinger equation. *Optik*, 167, 150-156.
- [11] Veerasha, P., Prakasha, D. G., Baskonus, H. M. 2019. Novel simulations to the time-fractional Fisher's equation. *Mathematical Sciences*, 13(1), 33-42.
- [12] Veerasha, P., Prakasha, D. G., Baskonus, H. M. 2019. New numerical surfaces to the mathematical model of cancer chemotherapy effect in Caputo fractional derivatives. *Chaos: An Interdisciplinary Journal of Nonlinear Science*, 29(1), 013119.
- [13] Caponetto, R., Dongola, G., Fortuna, L., Gallo, A. 2010. New results on the synthesis of FO-PID controllers. *Communications in Nonlinear Science and Numerical Simulation*, 15(4), 997-1007.
- [14] Prakash, A., Veerasha, P., Prakasha, D. G., Goyal, M. 2019. A homotopy technique for a fractional order multi-dimensional telegraph equation via the Laplace transform. *The European Physical Journal Plus*, 134, 1-18.
- [15] Mohand, M., Mahgoub, A. 2017. The new integral transform "Mohand Transform". *Advances in Theoretical and Applied Mathematics*, 12(2), 113-120.
- [16] Aggarwal, S., Sharma, N., Chauhan, R. 2018. Solution of linear Volterra integral equations of second kind using Mohand transform. *International Journal of Research in Advent Technology*, 6(11), 3098-3102.

- [17] Aggarwal, S., Gupta, A. R., Singh, D. P., Asthana, N., Kumar, N. 2018. Application of Laplace transform for solving population growth and decay problems. *International Journal of Latest Technology in Engineering, Management & Applied Science*, 7(9), 141-145.
- [18] Sathya, S., Rajeswari, I. 2018. Applications of Mohand transform for solving linear partial integro-differential equations. *International Journal of Research in Advent Technology*, 6(10), 2841-2843.
- [19] Kumar, P. S., Gomathi, P., Gowri, S., Viswanathan, A. 2018. Applications of Mohand transform to mechanics and electrical circuit problems. *International Journal of Research in Advent Technology*, 6(10), 2838-2840.
- [20] Kumar, P. S., Saranya, C., Gnanavel, M. G., Viswanathan, A. 2018. Applications of Mohand transform for solving linear Volterra integral equations of first kind. *International Journal of Research in Advent Technology*, 6(10), 2786-2789.
- [21] Zubik-Kowal, B. 2000. Chebyshev pseudospectral method and waveform relaxation for differential and differential-functional parabolic equations. *Applied numerical mathematics*, 34(2-3), 309-328.
- [22] Alkan, A. 2022. Improving Homotopy Analysis Method with An Optimal Parameter for Time-Fractional Burgers Equation. *Karamanoğlu Mehmetbey Üniversitesi Mühendislik ve Doğa Bilimleri Dergisi*, 4(2), 117-134.
- [23] Jackiewicz, Z., Zubik-Kowal, B. 2006. Spectral collocation and waveform relaxation methods for nonlinear delay partial differential equations. *Applied Numerical Mathematics*, 56(3-4), 433-443.
- [24] Mead, J., Zubik-Kowal, B. 2005. An iterated pseudospectral method for delay partial differential equations. *Applied numerical mathematics*, 55(2), 227-250.
- [25] Abazari, R., Ganji, M. 2011. Extended two-dimensional DTM and its application on nonlinear PDEs with proportional delay. *International Journal of Computer Mathematics*, 88(8), 1749-1762.
- [26] Abazari, R., Kilicman, A. 2014. Application of differential transform method on nonlinear integro-differential equations with proportional delay. *Neural Computing and Applications*, 24, 391-397.
- [27] Tanthanuch, J. 2012. Symmetry analysis of the nonhomogeneous inviscid Burgers equation with delay. *Communications in Nonlinear Science and Numerical Simulation*, 17(12), 4978-4987.
- [28] Sakar, M. G., Uludag, F., Erdogan, F. 2016. Numerical solution of time-fractional nonlinear PDEs with proportional delays by homotopy perturbation method. *Applied Mathematical Modelling*, 40(13-14), 6639-6649.
- [29] Biazar, J., Ghanbari, B. 2012. The homotopy perturbation method for solving neutral functional-differential equations with proportional delays. *Journal of King Saud University-Science*, 24(1), 33-37.
- [30] Chen, X., Wang, L. 2010. The variational iteration method for solving a neutral functional-differential equation with proportional delays. *Computers & Mathematics with Applications*, 59(8), 2696-2702.
- [31] Singh, B. K., Kumar, P. Fractional variational iteration method for solving fractional partial differential equations with proportional delay. *International journal of differential equations*, 2017, 2017.
- [32] Khalil, R., Al Horani, M., Yousef, A., Sababheh, M. 2014. A new definition of fractional derivative. *Journal of computational and applied mathematics*, 264, 65-70.
- [33] Abdeljawad, T. 2015. On conformable fractional calculus. *Journal of computational and Applied Mathematics*, 279, 57-66.
- [34] Ala, V., Demirbilek, U., Mamedov, K. R. 2020. An application of improved Bernoulli sub-equation function method to the nonlinear conformable time-fractional SRLW equation. *AIMS Mathematics*, 5(4), 3751-3761.
- [35] Gözütok, U., Çoban, H., Sağıroğlu, Y. 2019. Frenet frame with respect to conformable derivative. *Filomat*, 33(6), 1541-1550.